Frequency and concentration windows for the electric activation of a membrane active transport system

Vladislav S. Markin and Tian Y. Tsong
Department of Biochemistry, University of Minnesota, St. Paul, Minnesota 55108 USA

ABSTRACT Previous work has shown that a simple four-state membrane transport system can interact with an oscillating electric field to become an active transport system if there is charge translocation associated with conformational changes of the transporter and if affinities of the transporter for the ligand on the two sides of membrane are different. The relationship between the transport flux and both the frequency of the applied field and the concentration of ligand have been examined based on the following assumptions: the rate of the electroconformational change of the transporter is much greater than that of the ligand association/dissociation reaction, and the oscillating electric field has a large amplitude. It was found that the transport flux depends strongly on the frequency of the field and on the concentration of the ligand and it displays a window of broad bandwidth both on the frequency and the concentration axes. The maximum concentration gradient, or the static head, which can be supported by this mechanism is shown to be constant for field frequencies smaller than the rate of the electroconformational change. The static head value diminishes completely when the field frequency exceeds the rate of the conformational change. The presence of an optimal field frequency has been shown experimentally in several membrane enzyme systems. The theory was applied to the description of Rb and Na pumping in human erythrocytes stimulated by an AC field. The prediction of a window for a ligand concentration and the static head value may be tested experimentally. In addition, the rate constants and the equilibrium constants of the four state model can be determined by measuring positions of windows, fluxes, and static head values under different experimental conditions. These results are equally applicable to the oscillation of pressure, membrane tension, substrate concentration, or temperature if these external parameters can induce functionally relevant conformational changes of the transporter.

INTRODUCTION

It has previously been shown that oscillating electric fields (in the range of 10 V/cm, 1–10^6 Hz) which induce transmembrane potentials comparable in magnitude to those of the endogenous potentials of cell membranes can cause Na,K-ATPase to pump K^+, Rb^+, and Na^+ up their concentration gradients and mitochondrial ATPase to synthesize ATP, in the absence of other energy sources (1–5). Recently, an electroconformational coupling model for biological free energy transduction (6) by means of the electrochemical potential gradient of an ion (7, 8) has been proposed (9–14). In this model, a membrane enzyme with several conformational states of different polarization (sum of electric charges and dipoles), is driven by the periodic field to oscillate among its conformational states within the catalytic cycle, and in doing so it enables the enzyme to capture energy from the applied field to drive the reaction away from the chemical equilibrium. Electroconformational coupling is an example of oscillatory coupling which is frequently reported in the literature (15–21). These oscillatory reactions, either spontaneous or enforced, play vital functions in biological regulation and energy and signal transduction. We have examined the thermodynamic basis of the transduction of electric energy by a generalized membrane transport system and found conditions for maximum energy transfer (22, 23). Among other conditions, it was found that the conformational changes of the transporter must be at a rate much faster than those of the transport reactions and the field oscillation to achieve maximal efficiency. In addition, the frequency of the AC field must not exceed the rate of the conformational transitions. For this reason the analysis in the papers (22, 23) was carried out only for the frequencies which do not exceed the rate of the conformational transitions.

It was found experimentally (1, 3), however, that the frequency dependence of the active flux in an AC field is a nonmonotonous one. Fig. 1, taken from Liu et al. (3), presents the frequency dependence of electric field stimulated pump transport of Rb^+ and Na^+ in human red blood cells. The AC activation of the Rb^+ and Na^+ pumping mode have optimum frequencies of $\sim$1 kHz and 1 MHz which has not yet been theoretically described.

Dr. Markin is a visiting scholar from Frumkin Institute of Electrochemistry, Acad. Sci. USSR, Moscow, USSR 117071.
Address correspondence to Dr. Tsong at University of Minnesota.

0006-3495/91/06/1308/09 $2.00

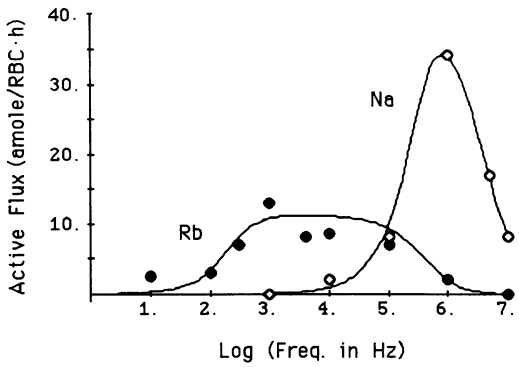

FIGURE 1 Experimental frequency dependence of the Rb^+ pumping and Na^+ pumping in RBC stimulated by AC field of 20 V/cm. Data taken from reference 3. Curves are drawn according to Eq. 26 with the following parameters. For Rb^+: $k_{14} = 1.25\ 10^3\ s^{-1}$, $\beta = 10{,}000$, $A(1 - K_{14})/(1 + A) = 1.25\ 10^{-2}$. For Na^+: $k_{14} = 1.58\ 10^6\ s^{-1}$, $\beta = 80$, $A(1 - K_{14})/(1 + A) = 3.4\ 10^{-5}$. The number of ATPase-molecules per RBC used for the calculation was 200.

Although the theoretical existence of an optimal frequency for the conversion of electric energy has been demonstrated by numerical analysis (11, 24), the relationship between kinetic characteristics of the transport scheme and the frequency of the AC field remained unclear. To approach this problem, we have investigated fluxes as a function of frequency in three frequency ranges so that the total frequency range is covered. We calculated the membrane active flux generated by the AC field and the static head which can be maintained by this mechanism. It was found that the active flux has an optimum both on the frequency and the concentration axes. The parameters of optimum frequency and concentration window were determined.

MEMBRANE TRANSPORT MODEL

Kinetic scheme

The simplest carrier mechanism is described by the four state model 1, where the transporter expressed in T, the ligand in A, and the rate constants, k_{ij}, are specified (25):

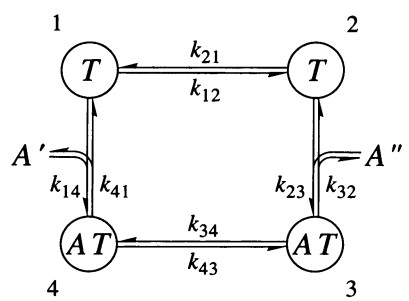

(1)

Rate constants k^*_{14} and k^*_{23} are marked with asterisks to emphasize that they have dimensions which differ from the dimensions of other rate constants in this scheme. This is because the flux of the particles of A across the membrane surface is given by the equation

$$j = k^*_{14} c'_A(T_1) - k_{41}(AT_4). \tag{2}$$

Here c'_A is the concentration of particles of A in the left-hand solution, and the (T_1) and (AT_4) are the concentrations of the corresponding species in the membrane. If the term c'_A has the dimension of volume concentration, say, moles per meter^{-3}, then it is obvious that the rate constants k^*_{14} and k_{41} have different dimensions. To avoid this inconvenience we shall change to a dimensionless relative concentration A', so that the rate constants k_{14} and k_{41} have the same dimensions. The same is true for the right side of the membrane with conventional concentration c'_A and association reaction rate constant k^*_{23}.

To switch from dimensional to dimensionless concentration A, we have to normalize the conventional concentration c_A by some characteristic concentration c^*_A. As follows from the mathematical analysis, the characteristic concentration c^*_A should be defined as

$$c^*_A = \sqrt{\frac{k_{41}k_{32}}{k^*_{14}k^*_{23}}}. \tag{3}$$

Therefore,

$$A = c_A/c^*_A \tag{4}$$

and

$$k_{14} = k^*_{14}\, c^*_A \tag{5}$$

$$k_{23} = k^*_{23}\, c^*_A. \tag{6}$$

Now all the rate constants in the kinetic Scheme 1 have the same dimension of $1/s$ and the concentration A is presented in relative units. In the following presentation we shall maintain this convention.

Antisymmetric transporter

A particular case of Scheme 1, called the antisymmetric transporter, is defined by assigning the following conditions to the rate constants of the surface reactions,

$$k_{14} = k_{32} \qquad k_{41} = k_{23} \tag{7}$$

and conformation transitions,

$$k_{12} = k_{34}, \qquad k_{21} = k_{43} \tag{8}$$

and to the equilibrium constants,

$$K_{14} = K_{12} = K_{32} = K_{34}. \tag{9}$$

When these conditions are met, Scheme 1 can be described with only two rate constants, k_{12} and k_{14}, and one equilibrium constant, K_{14}. All the others rate constants and equilibrium constants can be expressed via these three. In this case the kinetic equations are drastically simplified.

If the equilibrium constant K_{14} ($= k_{41}/k_{14}$) is much smaller (or greater) than unity, i.e., $K_{14} \ll 1$ or $K_{14} \gg 1$, the case is strongly antisymmetric. In such a case, the equations can further be simplified and the active transport phenomenon will become more pronounced. Where these special conditions are applied will be mentioned explicitly.

Active transport

As before (22, 23) we assume that A is uncharged but the transitions between T_1 and T_2 and between AT_3 and AT_4 involve a change of polarization of the protein (or equivalently, the intramolecular movement of charge, q, across the membrane), and the system is responsive to an electric pertubation (electric potential of ϕ). The state occupancies of the transporter at equilibrium will satisfy

$$T_1/T_2 = K_{12}e^{-\Psi}, AT_4/AT_3 = K_{43}e^{-\Psi}, \quad (10)$$

where $K_{12} = k_{21}/k_{12}$, $K_{43} = k_{34}/k_{43}$ are the equilibrium constants of the conformational change of the unloaded and loaded carrier at zero electric potential and $\psi = q\phi/RT$.

In general, the kinetic behavior of the transporter 1 can be simulated by analytically solving the four differential equations for Scheme 1 (24, 25).

The rate constants of consecutive steps in Scheme 1 determine the overall rate of energy transduction. One of them can be presented as the rate of the ligand/transporter interaction k_{chem} on the two sides of membrane which is given by the terms $(k_{14}A' + k_{41})$ or $(k_{23}A'' + k_{32})$. The second is the rate of conformational transitions of the transporter k_{conf} which is given by two values $(k_{12} + k_{21})$ and $(k_{43} + k_{34})$ for the protein unloaded or loaded with ligand A. In the presence of an electric field the conformational rate constants will include additional electrical terms $\lambda = \exp(\psi/2)$. We shall consider square-wave potential oscillations with the amplitude ψ_0. Therefore, the conformational relaxation rates k_{conf} in one half-period will be given by $(\lambda k_{12} + k_{21}/\lambda)$ and $(\lambda k_{43} + k_{34}/\lambda)$ and in the second half-period by $(k_{12}/\lambda + \lambda k_{21})$ and $(k_{43}/\lambda + \lambda k_{34})$.

As was shown earlier (22, 23), for active transport to occur it is necessary that the affinity of the transporter for the transported solute is different at the two sides of the membrane and the conformational changes are much faster than binding rates. We accept here this condition.

A schematic illustration of the energetics of the active pumping process was previously presented (23). We shall restrict the subsequent discussion to large amplitude field (meaning large amplitude interaction energy between the field and the enzyme conformation), such that all enzyme binding sites would be facing either right or left depending on the sign of the field. This allows us to obtain analytic expressions for flux generated by electric field and for the static head achieved in the quasi-equilibrum.

ACTIVE FLUX; FREQUENCY DEPENDENCE

By using these limiting conditions, transport flux of Scheme 1 has been solved analytically for square-wave of large oscillations amplitude ψ_0. When analyzing the frequency dependence of active transport we shall distinguish three frequency domains: low (l), moderate (m), and high (h). The low frequency domain covers the frequencies between zero and the rate of surface chemical reactions k_{chem}, the moderate frequency domain covers the frequencies between the rates of surface chemical reactions k_{chem} and conformational transitions k_{conf}, and high frequency domain exceeds the rate of conformational transitions. Later we shall give a more strict quantitative definition of the borders between these domains and define conditions for liking these domains.

If membrane potential is zero, there is only passive downhill flux which for arbitrary values of rate constants is given by

$$J_{passive} = \frac{k_{23}k_{41}K_{43}(A' - A'')}{[(k_{32} + k_{41}K_{43})(1 + K_{12}) + (k_{32}A'' + k_{14}A'K_{12})(1 + K_{43})]}. \quad (11)$$

In the presence of membrane potential square-wave oscillations, if these oscillations are large enough, the flux of particles of A across the membrane can be calculated analytically in two neighboring domains simultaneously, either in low and moderate frequency domains or in moderate and high frequency domains.

Low and moderate frequency domains

The solution in low and moderate frequency domains was described elsewhere (22, 23). For arbitrary values of

rate constants the result is

$$J_{lm} = \frac{1}{2\theta}\frac{k_{32}k_{14}A' - k_{41}k_{23}A'')}{(k_{41} + k_{14}A')(k_{32} + k_{23}A'')} \times \frac{\{1 - \exp[-(k_{32} + k_{23}A'')\theta]\}}{\{1 - \exp[-(k_{41} + k_{14}A')\theta]\}} \times \frac{\{1 - \exp[-(k_{41} + k_{14}A')\theta]\}}{\{1 - \exp[-(k_{41} + k_{14}A' + k_{32} + k_{23}A'')\theta]\}}, \quad (12)$$

where $\theta = 1/2f$.

Eq. 12 gives the frequency dependence of the average flux of A at low and moderate frequencies and can be explained as follows. In the low-frequency domain, the flux simplifies to

$$J_L = \frac{(K_{41}A' - K_{32}A'')}{(1 + K_{41}A')(1 + K_{32}A'')} f, \quad (13)$$

where K_{41} is the association constant for the left side of the membrane and K_{32} is the association constant for the right side. This result demonstrates that the flux proportional to the frequency with a slope that depends only on the association constants and the concentrations. In the moderate frequency domain the flux simplifies to

$$J_m = \frac{1}{2}\frac{(K_{41}A' - K_{32}A'')}{(1 + K_{41}A')/k_{32} + (1 + K_{32}A'')/k_{41}}, \quad (14)$$

which is independent of frequency. Hence, in this domain the flux displays a plateau. In the antisymmetric case it will be

$$J_m = \frac{k_{14}(A' - K_{14}^2A'')}{2(1 + K_{14} + A' + K_{14}A'')}. \quad (15)$$

The crossing of two asymptotes J_l and J_m determines the border between these two domains:

$$f_{lm} = \frac{1}{2}\frac{(1 + K_{41}A')(1 + K_{32}A'')}{(1 + K_{41}A')/k_{32} + (1 + K_{32}A'')/k_{41}}. \quad (16)$$

It is still a general case with respect to the values of rate constant. In the case of an antisymmetric transporter and equal concentrations $A' = A'' = A$ this expression becomes

$$f_{lm} = \frac{k_{14}(K_{14} + A)(1 + K_{14}A)}{2(1 + A)(1 + K_{14})}. \quad (17)$$

Note that this characteristic frequency is proportional to the only rate constant k_{14} preserved in this expression. It means that k_{14} becomes the "natural" scale for the frequency f. Subsequently we shall use the reduced dimensionless frequency $F = f/k_{14}$.

To make reasonable estimates for the characteristic frequency f_{lm} let us consider the case of strong antisymmetry. If K_{14} is small and A is of the order of unity, the expression simplifies to:

$$\frac{f_{lm}}{k_{14}} = \frac{A}{2(1 + A)}. \quad (18)$$

For $A = 1$ this is ¼. For the static head with $A' = K_{14}^2A'' = 1$ the dimensionless boundary frequency determined from Eq. 16 would be ½. Therefore, even for a very broad range of concentrations, the boundary between two domains is rather stable and approximated by the chemical reaction relaxation rate k_{chem}.

Thus, in the first two frequency domains, the flux initially increases linearly with frequency (Fig. 2, *curve a*) until the frequency approaches f_{lm}, and then levels off reaching the plateau described by Eq. 14.

Moderate and high frequency domains

For the frequencies which are comparable to or higher than the rate of conformational relaxation k_{conf} (where frequency considerably exceeds the rate of chemical reaction k_{chem}) the solution can be simplified because the sum of the population of states T_1 and T_2 does not change considerably in the cycle of the oscillation. The same is true for the sum of the populations of states AT_3 and AT_4.

To make the final results more obvious we consider the antisymmetric transporter as defined by Eqs. 7–9. Then the flux at moderate and high frequencies can be presented as

$$J_{mh} = f\frac{k_{14}[(\theta - H)^2A' - (\theta + H)^2K_{14}^2A'']}{(1 + A')(\theta - H) + K_{14}(1 + A'')(\theta + H)}, \quad (19)$$

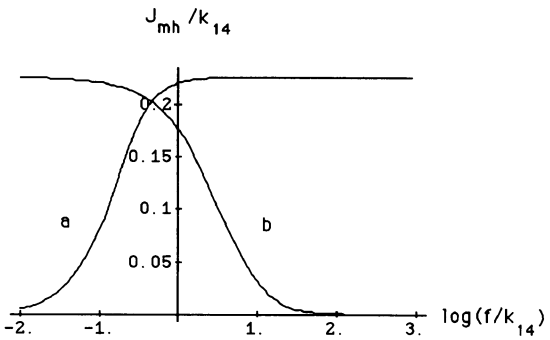

FIGURE 2 Frequency dependence of flux J_{lm} (*curve a*) drawn according to Eq. 12 and J_{mh} (*curve b*) for the antisymmetric transporter plotted according to Eq. 18. Equilibrium constant K_{14} equals 0.1, concentrations $A' = A'' = 1$ and $\beta = 100$.

—where

$$H = (\tau_{21} - \tau_{12}) \frac{[1 - \exp(-\theta/\tau_{12})]\,[1 - \exp(-\theta/\tau_{21})]}{[1 - \exp(-\theta/\tau_{12} - \theta/\tau_{21})]} \quad (20)$$

$$\tau_{12} = 1/(\lambda k_{12}) \text{ and } \tau_{21} = 1/(\lambda k_{21}). \quad (21)$$

Note that the Eq. 19 depends on the amplitude of membrane potential oscillations via the term λ.

Eq. 19 gives the expression for the flux J_{mh} as a function of frequency. This flux decreases with the frequency (Fig. 2, *curve b*). In the moderate frequency domain this flux approaches the maximum value which coincides with the plateau J_m displayed in this region by the flux J_{lm} as determined by Eq. 14. In the high frequency domain the flux decreases with frequency and finally reaches the level

$$J_h(\infty) = \frac{k_{41}(A' - A'')}{(1 + K_{14})(2 + A' + A'')}. \quad (22)$$

It would be useful to evaluate the expansion of the flux (Eq. 19) into series in the power of $1/f$. This expansion is rather cumbersome but it simplifies for level flow when $A' = A'' = A$. The first nonvanishing term is

$$J_h = \frac{\beta^2 k_{41}(1 - K_{14})}{96\,(1 + A)} \left|\frac{k_{14}}{f}\right|^2, \quad (23)$$

where $\beta = \lambda k_{12}/k_{14}$. One can see that the flux decreases with the second power of frequency.

The characteristic frequency f_{mh}, which separates two regions, can be defined as a point where the high frequency approximation of the flux 23 reaches a plateau level J_m as determined by Eq. 21. The resulting equation is

$$\frac{\beta^2 k_{41}(1 - K_{14})}{96\,(1 + A)} \left|\frac{k_{14}}{f}\right|^2 = \frac{k_{14} A (1 - K_{14})}{2\,(1 + A)} \quad (24)$$

and one can find the characteristic frequency

$$\frac{f_{mh}}{k_{14}} = \frac{\beta}{4}\sqrt{\frac{K_{14}}{3A}}. \quad (25)$$

The boundary between the moderate and high frequency domain is normally close to the relaxation rate of the conformational transition k_{conf}.

Flux in the total frequency range

Because the fluxes J_{lm} and J_{mh} have the same values in the moderate frequency domain, we can combine these two functions to describe the flux for the total frequency range. This approximation can be presented as

$$J_{lmh} = \frac{J_{lm} J_{mh}}{J_m}. \quad (26)$$

Hence, at the low frequencies the flux is given by J_{lm}, at high frequencies it is J_{mh}, and at moderate frequencies it is approximated by the product which is close to the plateau J_m. The plots of this function for $K_{14} = 0.1, A = 1$, and different values of parameter β are given in Fig. 3. The second curve in this plot corresponds to $\beta = 100$ and is a product of curves for J_{lm} and J_{mh} presented in Fig. 2. This function displays a sharp maximum because the width of the moderate frequency domain is small: the boundaries have the coordinates $\log(f_{lm}/k_{14}) = -0.56$ and $\log(f_{mh}/k_{14}) = 0.66$. Hence the difference between the two coordinates only slightly exceeds unity.

Eq. 26 is better the larger the distance between these boundary points (larger parameter). As this distance increases, the maximum becomes broader as shown in Fig. 3. The position of this maximum on the frequency axis can be expressed as

$$f_{max} = \sqrt{f_{lm}\, f_{mh}}. \quad (27)$$

CONCENTRATION DEPENDENCE

Two types of concentration dependence shall be distinguished: one-side and two-side concentration dependence. In the first case, the concentration is changed at one side, while the other is kept constant. In this case the static head can be observed. In the second case the concentrations of A' and A'' are equal and change at the same rate. The flux in this case is called level flow. We shall consider both cases.

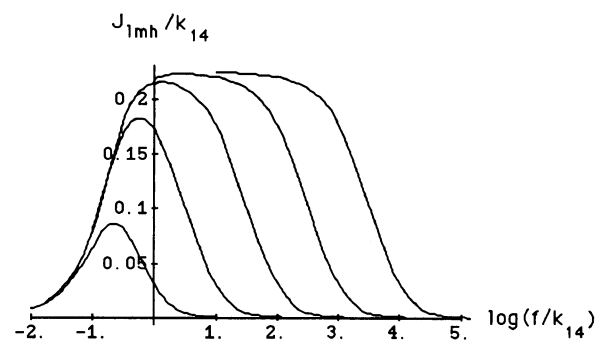

FIGURE 3 Frequency dependence of flux J_{lmh} for the antisymmetric transporter drawn according to Eq. 26 with equilibrium constant $K_{14} = 0.1$ and concentrations $A' = A'' = 1$. The curves from left to right have the following values of parameter β: 10; 100; 1,000; 10,000; and 100,000.

Static head

The dependence of flux on the concentration of A'' with the concentration of A' being kept constant is presented in Fig. 4 for $A' = 1$, $K_{14} = 0.1$, $\beta = 1000$ and different frequencies. The flux from left to right is considered positive, therefore, it decreases with increasing concentration of A''. The curves cross the abscissa and go to the negative region indicating a change of the direction of flux and concomitantly a change of the direction of energy transduction as was previously described (22, 23). Here the active transport system is transformed into an electrical generator which can use the energy stored in the form of a concentration gradient to produce spontaneous or enforced electrical oscillations.

The points where the curves cross the abscissa are the static head points, where active pumping stops and the system is in a state of quasi-equilibrium. The ratio of concentrations A''/A' at the static head can be determined from the equation $J_{lmh} = 0$, which gives

$$\left(\frac{A''}{A'}\right)_{sh} = \frac{(\theta - H)^2(K_{14})^2}{(\theta + H)^2}. \tag{28}$$

This represents the theoretical limit of the concentration gradient that can be supported by the transport system. In previous work (22, 23) the static head was found in the domains of low and moderate frequencies only where

$$(A''/A')_{sh} = K_{41}/K_{32} \tag{29}$$

or in the case of antisymmetric transporter

$$(A''/A')_{sh} = K_{41}^2. \tag{30}$$

In Fig. 4 this situation corresponds to the limiting curve 1 with dimensionless frequency $f/k_{14} = 1$. The static head here is equal to 100. Indeed, this curve crosses the abscissa at the point, $\log A'' = 2$. This means that the transport system can create and maintain a 100-fold concentration gradient of neutral particles across membrane.

For low and moderate frequencies the concentration gradient which can be supported by the transport system is determined solely by the thermodynamic parameters of this system. The static head point concentration ratio, Eqs. 29 or 30, in these regions (or at least in the domain of low frequency if the width of moderate frequency domain is not large enough) does not depend on concentrations or frequency. But the general expression, Eq. 28, depends on both of these parameters so when the frequency increases the static head decreases until it disappears completely, which means $(A''/A')_{sh} = 1$. The dependence of static head $(A''/A')_{sh}$ on frequency is presented in Fig. 5 with the parameters $A' = 1$, $K_{14} = 0.1$, and $\beta = 1{,}000$. In the left part of the plot the curve reaches 100 and at the right side it levels off at 1.

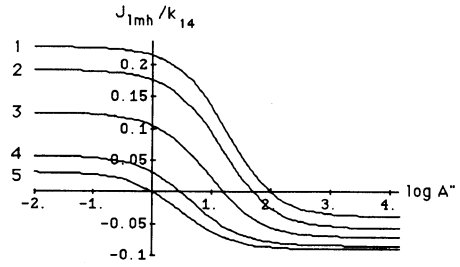

FIGURE 4 Flux J_{lmh} as a function of one-side concentration A''. The following parameters are used: $K_{14} = 0.1$, $\beta = 1{,}000$, and $A' = 1$. Dimensionless frequency f/k_{14} was changing with the curves: 1) 1; 2) 10; 3) 30; 4) 100; and 5) 1,000. The points where the curves cross the abscissa give the static heads which decreases with increasing frequency.

Level flow

The two-side concentration dependence of active flux where concentrations are equal to each other is called level flow. The flux is given by the general Eq. 26 with $A' = A'' = A$. For the case of the antisymmetric transporter, and low frequency, this flux can be derived from Eq. 13:

$$J_l = \frac{f(1 - K_{14}^2)A}{(K_{14} + A)(1 + K_{14}A)}. \tag{31}$$

This function of concentration has a maximum at the point where $A = 1$ and the absolute value of this function depends on the frequency f.

For moderate frequency the level flux in the case of

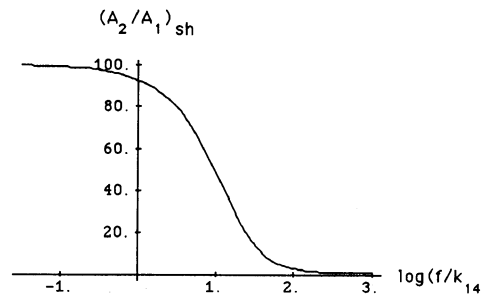

FIGURE 5 Frequency dependence of the static head. Parameters $K_{14} = 0.1$ and $\beta = 1{,}000$.

antisymmetric transporter can be derived from Eq. 15 as

$$J_m = \frac{k_{14}(1 - K_{14})A}{2(1 + A)}. \quad (32)$$

The flux gradually increases as A increases but then reaches a plateau with a characteristic transition point of $A = 1$. This function does not depend on frequency while it is confined to the moderate frequency domain.

Therefore one could expect the level flux as a function of concentration to increase until it reaches a plateau and then to remain on this plateau. But Fig. 6 presents another dependence at high concentrations of A. The curves are bell-shaped (1 and 2) or display the broad maximum (3 and 4) but finally decrease to zero. This behavior will be analyzed in the next section.

OPTIMUM WINDOW

The boundaries between different frequency domains as presented by Eqs. 17 and 25 are concentration dependent. If f_{lm} and f_{mh} are plotted for antisymmetric transporter as functions of A, we obtain Fig. 8 with the parameters $K_{14} = 0.1$ and $\beta = 100$. The upper curve gives f_{mh} and the lower curve gives f_{lm}. These lines divide the plane $A - f$ into domains corresponding to low, moderate, and high frequencies. The structure of this plane is such that at low concentrations all three domains are available. If the concentration is increased then the width of the moderate frequency domain decreases and eventually this domain disappears.

The crossing point of these two lines may be found by solving the equation $f_{lm} = f_{mh}$. For large β, the critical concentration is obtained when the moderate frequency domain disappears:

$$A_{crit} = \sqrt[3]{\frac{\beta^2 (1 + K_{14})^2}{12 K_{14}}}. \quad (33)$$

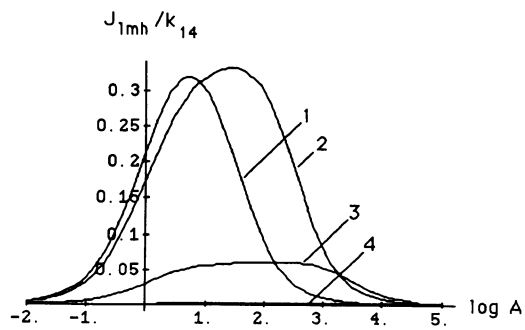

FIGURE 6 Concentration dependence of flux J_{lmh} for $K_{14} = 0.1$, $\beta = 1{,}000$, and $A' = A'' = 1$. The parameter of the curves is dimensionless frequency f/k_{14}: 1) 1; 2) 10; 3) 100; and 4) 1,000.

The coordinate of this point on the frequency axis is

$$\frac{f_{crit}}{k_{14}} = \frac{1}{4}\sqrt[3]{\frac{2\beta^2 K_{14}^2}{3(1 + K_{14})}}. \quad (34)$$

The existence of a crossing point indicates that it is possible to pass from the low frequency to the high frequency domain without crossing the moderate frequency domain. This point is somewhat analogous to the critical point in the phase transition theory. In our case it means that for the large concentrations there is no plateau of the frequency dependence for level flux.

This explains the observation made in the end of the preceding section. When we investigate the concentration dependence of flux, even if at low concentrations, we start at the point belonging to the moderate frequency domain, when this concentration increases we inevitably leave this domain and enter either the low frequency or high frequency domain. In both cases the flux will decrease with concentration.

The division of the plane $f - A$ into different domains suggests that in some regions of this plane the energy transduction can proceed with the highest rate and efficiency. We shall call this region the optimum frequency and concentration window. This window must be somewhere in the moderate frequency domain. But it cannot include very low concentrations because as was demonstrated in the Eq. 32, the flux at low concentrations would be too low. The transition point between low and high fluxes is $A_{trans} = 1$.

Therefore the most promising region is the part of the moderate frequency domain in Fig. 7 to the right of the vertical line passing through $A = 1$ or $\log A = 0$. The position of maximum flux in this optimum window is of utmost interest. To avoid very cumbersome formulas we find this position approximately. The frequency coordi-

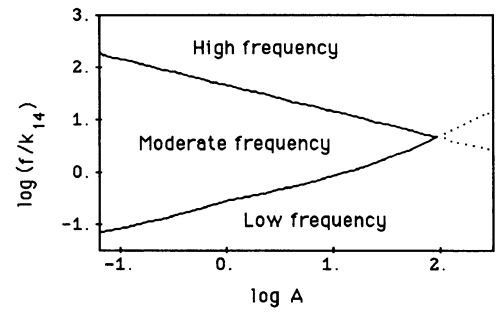

FIGURE 7 Frequency domains on the plane frequency-concentration. The upper curve is $f_{mh}(A)$ drawn according to the Eq. 25 and the lower curve is $f_{lm}(A)$ drawn according to the Eq. 18 with the parameters $K_{14} = 0.1$ and $\beta = 1{,}000$. These lines divide the plane $f - A$ into domains corresponding to low, moderate, and high frequencies.

nate of the maximum f_{max} must be close to f_{crit}. Hence

$$\frac{f_{max}}{k_{14}} = \frac{1}{4}\sqrt[3]{\frac{2\beta^2 K_{14}^2}{3(1+K_{14})}}. \quad (35)$$

The concentration corresponding to this maximum may be taken as the geometrical mean of A_{trans} and A_{crit}:

$$A_{max} = \sqrt[6]{\frac{\beta^2(1+K_{14})^2}{12K_{14}}}. \quad (36)$$

To check these predictions we present in Fig. 8 *A* the three-dimensional plot of level flux as a function of frequency and concentration. Parameters of this function are $K_{14} = 0.1$ and $\beta = 100$. This surface displays a rather sharp "hill." The position of this hill becomes clearer in Fig. 8 *B* where this function is presented as a density plot. The cross-mark on this plot shows the position of the top of the hill as calculated with Eqs. 35 and 36. These coordinates are $\{\log(f_{max}/k_{14}) = -0.008$ and $\log A_{max} = 0.667\}$. The cross-mark is located in the center of the window proving that Eqs. 35 and 36 give a good approximation.

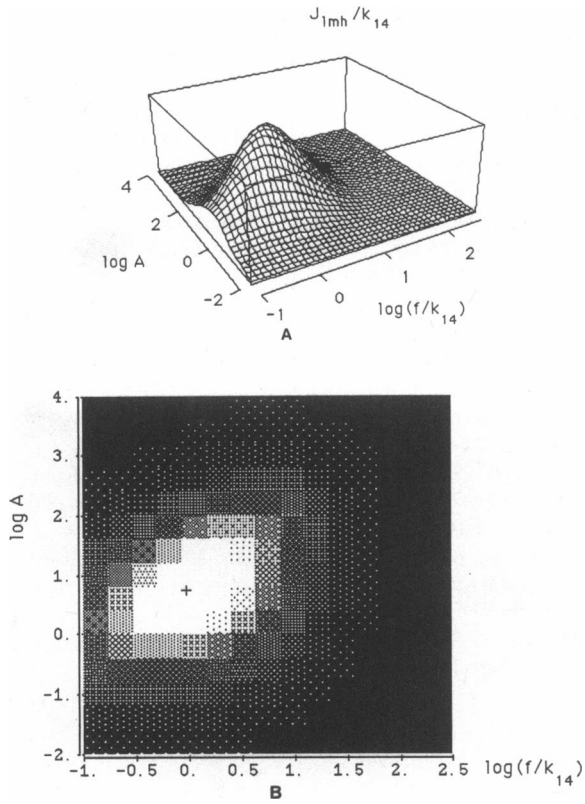

FIGURE 8 Flux J_{lmh} as a function of dimensionless frequency f/k_{14} and concentration $A' = A'' = A$ for $K_{14} = 0.1$ and $\beta = 100$. (*A*) Three-dimensional plot. (*B*) Optimum frequency and concentration window presented as a density plot. The height of the function $J_{lmh}(f, A)$ at each point is shown by the degree of shading. The cross marks the position of the maximum flux. It has the coordinates $\{\log(f_{max}/k_{14}) = -0.008$ and $\log A_{max} = 0.667\}$ which were calculated according to Eqs. 27 and 36.

DISCUSSION

We have demonstrated that the rate and the efficiency of energy transduction by the electroconformational couple mechanism can be optimized if the proper frequency and concentration "windows" are selected. In these windows the flux reaches the highest values as is shown by the three-dimensional plot in Fig. 8 *A*. The optimum frequency and concentration window is clearly presented in Fig. 8 *B*.

To illustrate this pheonomenon with a real biological experiment, we have used the data on AC field stimulation of Rb^+ and Na^+ pumping in human erythrocytes (3). These data are presented in the Fig. 1. As was described above, from this dependence, one can find the rate constant k_{14} which determines the left border of the optimum window on the frequency axis and β which determines the right border of the frequency window. For Rb^+ these parameters were found to be $k_{14} = 1.25 \times 10^3\ s^{-1}$ and $\beta = 10{,}000$, and for Na^+ they were $k_{14} = 1.58 \times 10^6\ s^{-1}$ and $\beta = 80$. If the number of ATPase molecules per RBC is 200, then the coefficient $A(1 - K_{14})/(1 + A)$ determing the magnitude of the fluxes may be calculated. For Rb it was 1.25×10^{-2} and for Na^+ it was 3.4×10^{-5}. In spite of the good coincidence of experimental points with the theoretical predictions this plot should be considered a qualitative example because the theory was developed for the pumping of neutral particles. We believe that the same mechanism should work in the case of ion pumping, though some additional features become important in the latter case (manuscript to be published).

If the concentration difference exceeds the static head, energy is transduced in the opposite direction, turning the transporter into a kind of electric field generator. The analysis of frequency dependence of the static head demonstrated that at small and moderate frequencies the static head is constant while at high frequencies it decreases and disappears completely. This means that energy can be absorbed from the AC field and stored in the form of a concentration gradient, if the external field oscillates with low and moderate frequencies only.

The results obtained here for the electrical oscillations are applicable to the oscillation of pressure, membrane tension, concentration, temperature etc. Many kinds of oscillations can become a driving force for pumping of neutral (23) or charged (manuscript submit-

ted for publication) particles up the gradient of their electrochemical potential and hence can be used by this mechanism in the process of energy transduction as a source of energy. For example, the acoustic signal transduction into membrane potential was recently analyzed in detail (see following paper).

We thank Carol J. Gross for help with manuscript.

This work was supported by an Office of Naval Research grant to Dr. Tsong.

Received for publication 8 November 1990 and in final form 20 February 1991.

REFERENCES

1. Serpersu, E. H., and T. Y. Tsong. 1983. Stimulation of an ouabain-sensitive Rb^+ uptake in human erythrocytes with an external electric field. *J. Membr. Biol.* 74:191–201.
2. Serpersu, E. H., and T. Y. Tsong. 1984. Activation of electrogenic Rb^+ transport of (Na, K)-ATPase by an electric field. *J. Biol. Chem.* 259:7155–7162.
3. Liu, D.-S., R. D. Astumian, and T. Y. Tsong. 1990. Activation of Na^+ and K^+ pumping modes of (Na,K)-ATPase by an oscillating electric field. *J. Biol. Chem.* 265:7260–7267.
4. Witt, H. T., E. Schlodder, and P. Graber. 1976. Membrane-bound ATP synthesis generated by an external electrical field. *FEBS (Fed. Eur. Biochem. Soc.) Lett.* 69:272–276.
5. Teissie, J. 1986. Adenosine 5'-triphosphate synthesis in *Escherichia coli* submitted to a microsecond electric pulse. *Biochemistry.* 25:368–373.
6. Mitchell, P. 1979. Keilin's respiratory chain concept and its chemiosmotic consequences. *Science (Wash. DC).* 206:1148–1159.
7. Stein, W. D. 1985. Transport and Diffusion across Cell Membranes. Academic Press. New York. 300 pp.
8. Drachev, A. L., V. S. Markin, and V. P. Skulachev. 1985. $\Delta\mu H$-buffering by Na^+ and K^+-gradients in bacteria. Model and experimental systems. *Biochim. Biophys. Acta.* 812:197–213.
9. Tsong, T. Y., and R. D. Astumian. 1986. Absorption and conversion of electric field energy by membrane bound ATPases. *Bioelectrochem. Bioenerg.* 15:457–475.
10. Astumian, R. D., and B. Robertson. 1989. Nonlinear effect of an oscillating electric field on membrane proteins. *J. Chem. Phys.* 91:4891–4901.
11. Robertson, B., and R. D. Astumian. 1990. Kinetics of multistate enzyme in a large oscillating field. *Biophys. J.* 57:689–696.
12. Astumian, R. D., P. B. Chock, T. Y. Tsong, and H. V. Westerhoff. 1989. Effects of oscillations and energy-driven fluctuations on the dynamics of enzyme catalysis and free energy transduction. *Phys. Rev. A.* 39:6416–6435.
13. Tsong, T. Y. 1990. Electrical modulation of membrane proteins: enforced conformational oscillations and biological energy and signal transductions. *Annu. Rev. Biophys. Biophys. Chem.* 19:83–106.
14. Weaver, J. C., and R. D. Astumian, 1990. The response of living cells to very weak electric fields: the thermal noise limit. *Science (Wash. DC).* 247:459–462.
15. Devreotes, P. N. 1989. *Dictyostelium discoideum:* a model system for cell-cell interactions in development. *Science (Wash. DC).* 245:1054–1058.
16. Knox, B. E., P. N. Devreotes, A. Goldbeter, and L. A. Segel. 1986. A molecular mechanism for sensory adaptation based on ligand-induced receptor modification. *Proc. Natl. Acad. Sci. USA.* 83:2345–2349.
17. Olson, E. S., and L. D. Smullin. 1989. Frequency tuning in the electroreceptive periphery. *Biophys. J.* 55:1191–1204.
18. Mandelkow, E., E. M. Mandelkow, H. Hotani, B. Hess, and S. C. Muller. 1989. Spatial patterns from oscillating microtubules. *Science (Wash. DC).* 246:1291–1293.
19. Toko, K., M. Souda, T. Matsuno, and K. Yamaguji. 1990. Oscillations of electrical potential along a root of a higher plant. *Biophys. J.* 57:269–279.
20. Okamura, N., and S. Ishiwata. 1988. Spontaneous oscillatory contraction of sarcomeres in skeletal myofibrils *J. Muscle Res. Cell Motil.* 9:111–119.
21. Li, Y.-X., and A. Goldbeter. 1989. Frequency specificity in intercellular communication. Influence of patterns of periodic signaling on target cell responsiveness. *Biophys. J.* 55:125–145.
22. Markin, V. S., T. Y. Tsong, D. Astumian, and B. Robertson. 1990. Energy transduction between a concentration gradient and an alternating electric field. *J. Chem. Phys.* 93:5062–5066.
23. Markin, V. S., T. Y. Tsong, D. Astumian, and B. Robertson. Membrane transporters as free energy transducers: optimization of energy transfer. *Sov. Biol. Membr.* In press.
24. Robertson, B., and R. D. Astumian. 1990. Michaelis-Menten equation for an enzyme in an oscillating electric field. *Biophys. J.* 58:969–974.
25. Markin, V. S., and Y. A. Chizmadzhev. 1974. Faciliated Ion Transport. Izdatelstvo 'Nauka', Moscow. 260 pp.